OPEN

Improved Readout-Segmented Echo-Planner Diffusion-Weighted Magnetic Resonance Imaging of Nasopharyngeal Carcinoma Using Simultaneous Multislice Acquisitions at 3 T

Qiao Li, MD,† TingTing Jiang, MM,*† TingTing Wang, MD, PhD,*† Yan Huang, MM,*† XiaoXin Hu, MM,* Ling Zhang, MSc,* Wei Liu, PhD,‡ CaiXia Fu, MSc,‡ and YaJia Gu, MD, PhD*†*

Purpose: This study systematically compared the images from readout-segmented echo-planar diffusion-weighted imaging (RESOLVE-DWI [RS-DWI]) and simultaneous multislice accelerated RESOLVE-DWI (SMS-RS-DWI) in patients with nasopharyngeal carcinoma (NPC) in qualitative and quantitative aspects.

Method: Forty-four patients with NPC were included. The RS-DWI and prototypic SMS-RS-DWI sequences were performed on all patients. Images were qualitatively evaluated by 4 independent radiologists using a 5-point Likert scale. For quantitative evaluation, the maximum and minimum diameters and the maximum tumor areas were determined for both DWI sequences and compared with the T2-weighted imaging (T2WI) to evaluate image distortions. The apparent diffusion coefficient was measured in the slice with the maximum tumor profile.

Results: The SMS-RS-DWI was superior to RS-DWI with respect to overall image quality (3.40 ± 0.53 vs 2.71 ± 0.48, $P < 0.0001$) and tumor edge sharpness (3.29 ± 0.65 vs 2.64 ± 0.47, $P < 0.0001$). Susceptibility artifacts were significantly less severe in SMS-RS-DWI than in RS-DWI (0.85 ± 0.57 vs 1.36 ± 0.57, $P < 0.0001$). There was no significant overestimation or underestimation of the tumor geometry using the SMS-RS-DWI or RS-DWI compared with T2WI. The quantitative analysis showed a slightly higher agreement for SMS-RS-DWI with T2WI than RS-DWI for maximum diameter, minimum diameter, and maximum tumor area. The apparent diffusion coefficient values showed no significant differences between the 2 DWI techniques ($P > 0.05$).

Conclusions: At 3 T, SMS-RS-DWI is a useful technique for diagnosing NPC. It substantially improves different aspects of image quality by providing higher spatial resolution and fewer susceptibility artifacts with more extensive anatomic coverage compared with RS-DWI.

Key Words: nasopharyngeal carcinoma, readout-segmented echo-planar diffusion-weighted imaging, simultaneous multislice accelerated readout-segmented echo-planar diffusion-weighted imaging

(*J Comput Assist Tomogr* 2022;46: 815–822)

Nasopharyngeal carcinoma (NPC) is characterized by distinct geographical distribution and is particularly prevalent in East and Southeast Asia.[1,2] Magnetic resonance imaging (MRI) is a conventional and essential tool for pretreatment staging and therapeutic strategy development in patients with NPC. Moreover, diffusion-weighted imaging (DWI) is sensitive to water molecule motion, making it a useful functional MRI technique to evaluate tissue viabilities and tumor behaviors. Diffusion-weighted imaging has the following clinical applications in NPC patients: (1) detects a lesion in the early stage,[3] (2) predicts or monitors the treatment response,[4–6] and (3) distinguishes recurrence and postirradiation changes.[7,8]

The traditional technique for DWI is the single-shot echo-planner imaging (SS-EPI). However, evaluating NPC with SS-EPI always showed magnetic susceptibility artifacts caused by susceptibility changes at tissue-air and tissue-bone interfaces of the skull base. The readout-segmented echo-planar diffusion-weighted imaging (RESOLVE-DWI [RS-DWI]) can provide a higher image quality in the head and neck areas by reducing susceptibility and T2* blurring artifacts with shorter echo-spacing and echo train duration in the phase-encoding directions.[9–11] The apparent diffusion coefficient (ADC) values of RS-DWI can serve as an effective imaging biomarker to assess the treatment responses in patients with NPC.[12]

Despite its considerably diagnostic value, the relatively long acquisition time of RS-DWI limits its applications in routine clinical work. Recently, simultaneous multislice (SMS) based on the blipped "Controlled Aliasing In Parallel Imaging Results In Higher Acceleration" (blipped CAIPIR-INHA) technique has been proposed as a better solution to reduce the scan time for simultaneous multiband radiofrequency excitations and multiple-slice acquisitions in a shared readout time. It was initially applied to SS-EPI and extended to RS-EPI.[13,14] Its application has been shown to substantially reduce the acquisition time while maintaining comparable or even improving image quality compared with a standard DWI.[15,16] Moreover, a recent study also proved that SMS acquisitions could be applied to RS-DWI in patients with head and neck lesions and healthy female volunteers.[17] However, to our knowledge, no study has evaluated the feasibility and effectiveness of SMS-RS-DWI focusing on NPC.

In the present study, we used the SMS technique to further increase the spatial resolution of RS-DWI with more extensive anatomic coverage. We systematically compared the SMS-RS-DWI to the RS-DWI in NPC patients with respect to qualitative and quantitative imaging aspects.

MATERIALS AND METHODS

Patients

This study was approved by the research ethics committee of the institution. From July 2020 to October 2020, patients with clinically diagnosed NPC all received nasopharyngeal MR examination, including conventional MRI, RS-DWI, and SMS-RS-DWI. The exclusion criteria for analysis were as follows: (1) severe susceptibility or motion artifacts on the DW images, and (2) small tumor volumes (anteroposterior diameter <5 mm) that

From the *Department of Radiology, Fudan University Shanghai Cancer Center; †Department of Oncology, Shanghai Medical College, Fudan University, Shanghai; and ‡MR Applications Development, Siemens Shenzhen Magnetic Resonance Ltd, Shenzhen, China.

Received for publication September 6, 2021; accepted January 15, 2022.

Correspondence to: YaJia Gu, MD, PhD, 270 Dong An Rd, 200032 Shanghai, China (e-mail: guyajia@126.com).

QL. and T.J. have contributed equally to this work.

The authors declare no conflict of interest.

DOI: 10.1097/RCT.0000000000001327

TABLE 1. MR Imaging Sequence Parameters

Parameter	T2WI	RS-DWI	SMS-RS-DWI
Field of view, mm^2	270 × 228	200 × 200	200 × 200
Matrix	384 × 288	118 × 118	144 × 144
Voxel size, mm^3	0.7 × 0.7 × 5.0	1.7 × 1.7 × 4.0	1.4 × 1.4 × 4.0
Slice thickness, mm	5.0	4.0	4.0
No. slices	22	15	30
b Value, s/mm^2	NA	50, 800	50, 800
Echo time, ms	78	56	58
Echo spacing, ms	13	0.36	0.36
Time to repeat, ms	2500.0	3100	3000
Bandwidth, Hz/px	260	963	694
Flip angle, deg	180	180	180
Parallel imaging factor	2	2	2
Slice acceleration	1	1	2
Acquisition time, min	1:35	3:17	3:08

could lead to challenges with the imaging analyses. Finally, 44 patients with NPC (34 men and 10 women; age range, 30–73 years; mean ± SD, 48.1 ± 12.4 years) were enrolled in the present study.

MR Protocol

Magnetic resonance imaging was performed using a 3T scanner (MAGNETOM Skyra; Siemens Healthineers, Erlangen, Germany) with a dedicated 20-channel head-neck synergic coil.

Detailed scan parameters of the turbo-spin-echo (TSE) T2-weighted imaging (T2WI) and the 2 DWI sequences are summarized in Table 1. In both the DWI sequences, a monopolar diffusion preparation according to the Stejska-Tanner scheme was used, and fat suppression was also performed using a spectral attenuated inversion recovery pulse. The T2WI served as the standard anatomic reference for quantifying the degree of imaging geometric distortion.

Image Analysis

The original Digital Imaging and Communications in Medicine sets were anonymized, and the MRI parameters were removed. To make sure all readers were blind to the diffusion sequences that they were evaluating, the DWI sequences were anonymous and named as sequences 1 and 2. All radiologists worked independently without others. All qualitative assessments and quantitative analysis of the images were performed using OsiriX 5.0 (OsiriX Foundation, Geneva, Switzerland). Image analysis was executed by 4 independent readers (2 junior radiologists with more than 3 years of experience in head and neck imaging, and 2 senior radiologists with more than 10 years of experience).

Qualitative Image Assessment

The readers independently ranked the RS-DWI and SMS-RS-DWI images for overall image quality, tumor edge sharpness, and susceptibility artifacts on a 5-point Likert scale.

First, overall image quality for DWI images was rated as follows: 0, nondiagnostic; 1, poor; 2, fair; 3, good; and 4, excellent. Second, the tumor edge sharpness was graded as follows: 0, no identification; 1, poorly identifiable, no clear anatomic border; 2, borders are identifiable and blurry; 3, good differentiability of borders, with only minor deficits; and 4, excellent differentiation of lesion borders. Third, susceptibility artifacts were graded as follows: 0, no artifacts; 1, minor artifacts with no impact on diagnostic evaluation; 2, moderate artifacts with slight impact on diagnostic evaluation; 3, severe artifacts with considerable impact on diagnostic evaluation; and 4, very severe artifacts that prevent the diagnostic evaluation of the lesion.

Quantitative Image Analysis

The anatomic agreements between different DWI techniques with T2WI were used to evaluate geometric distortion by performing quantitative analysis. The axial slice that covered the largest extent of the NPC tumor on TSE T2WI was selected. The maximum diameter was measured on this slice and the corresponding slices of the DWI sequences with a *b* value of 800 s/mm^2. The diameter perpendicular to the maximum diameter on the maximum slice was also measured as the minimum diameter. Regions of interest (ROIs) were manually drawn to contour the borders of the NPC tumors on the maximum slices during axial TSE T2WI, RS-DWI, and SMS-RS-DWI, avoiding the inclusion of air, macroscopic necrosis, and adjacent anatomical structures, such that the maximum tumor area could be analyzed.

The MR system automatically generated the ADC maps after data acquisition. Circular ROIs were manually drawn on the slices with the maximum NPC tumor profile in both the RS-DWI and SMS-RS-DWI ADC maps. Another 2 ROIs were placed on the upper and lower adjacent slices within the NPC tumors. All ROIs were carefully placed on the visually homogeneous parenchyma

TABLE 2. Interobserver Agreements of Qualitative Parameters

	SMS-RS-DWI			RS-DWI		
Imaging Parameter	$\kappa 1$	$\kappa 2$	$\kappa 3$	$\kappa 1$	$\kappa 2$	$\kappa 3$
Overall image quality*	0.718	0.845	0.704	0.705	0.814	0.771
Sharpness of tumor edges†	0.742	0.722	0.740	0.716	0.718	0.689
Susceptibility artifacts‡	0.845	0.871	0.821	0.676	0.738	0.691

$\kappa 1$: interobserver agreement of qualitative indicators between 2 junior radiologists; $\kappa 2$: interobserver agreement of qualitative indicators between 2 senior radiologists; $\kappa 3$: interobserver agreement of qualitative indicators between radiologists of different seniority.

*Five-point Likert scale from 0 (nondiagnostic) to 4 (excellent).

†Five-point Likert scale from 0 (no identification) to 4 (excellent differentiation of lesion borders).

‡Five-point Likert scale from 0 (no artifacts) to 4 (very severe artifacts that prevent the diagnostic assessment of the lesion).

TABLE 3. Interobserver Agreements of Quantitative Parameters

Imaging Parameter	SMS-RS-DWI			RS-DWI		
	ICC1	ICC2	ICC3	ICC1	ICC2	ICC3
Maximum diameter, mm	0.791 (0.496–0.913)	0.924 (0.816–0.968)	0.806 (0.679–0.932)	0.817 (0.559–0.924)	0.943 (0.864–0.977)	0.865 (0.812–0.926)
Minimum diameter, mm	0.956 (0.894–0.982)	0.966 (0.918–0.986)	0.936 (0.876–0.953)	0.954 (0.889–0.981)	0.949 (0.877–0.979)	0.962 (0.896–0.992)
Maximum tumor area, mm^2	0.928 (0.826–0.970)	0.955 (0.891–0.981)	0.957 (0.904–0.969)	0.932 (0.837–0.972)	0.959 (0.902–0.983)	0.934 (0.894–0.954)
ADC value	0.860 (0.663–0.942)	0.844 (0.624–0.935)	0.853 (0.645–0.913)	0.917 (0.799–0.965)	0.801 (0.540–0.921)	0.835 (0.647–0.939)

ICC1: interobserver agreement of quantitative indicators between 2 junior radiologists; ICC2: interobserver agreement of quantitative indicators between 2 senior radiologists; ICC3: interobserver agreement of quantitative indicators between radiologists of different seniority.

with a diameter of ~1 cm. The mean ADC values of these 3 ROIs were recorded for further analysis.

Statistical Analysis

All statistical analyses were performed using MedCalc software (version 19.3; Ostend, Belgium). A P value of <0.05 was considered statistically significant.

The interobserver agreements for quantitative indicators were analyzed by calculating the weighted κ coefficients. The interobserver agreements for qualitative indicators were evaluated using the interclass correlation coefficients (ICCs). The κ and ICC values of less than 0.2, 0.21 to 0.4, 0.41 to 0.6, 0.61 to 0.80, and greater than 0.8 were considered to indicate poor, fair, moderate, substantial, and excellent positive agreement, respectively. The consistency analyses between 2 junior radiologists and 2 senior radiologists were performed. The mean values of 2 radiologists with the same seniority were calculated for the consistency analyses between radiologists with different seniority.

All variables were expressed as mean ± SD. A Shapiro-Wilk W test was performed to test the normality of the data. The paired

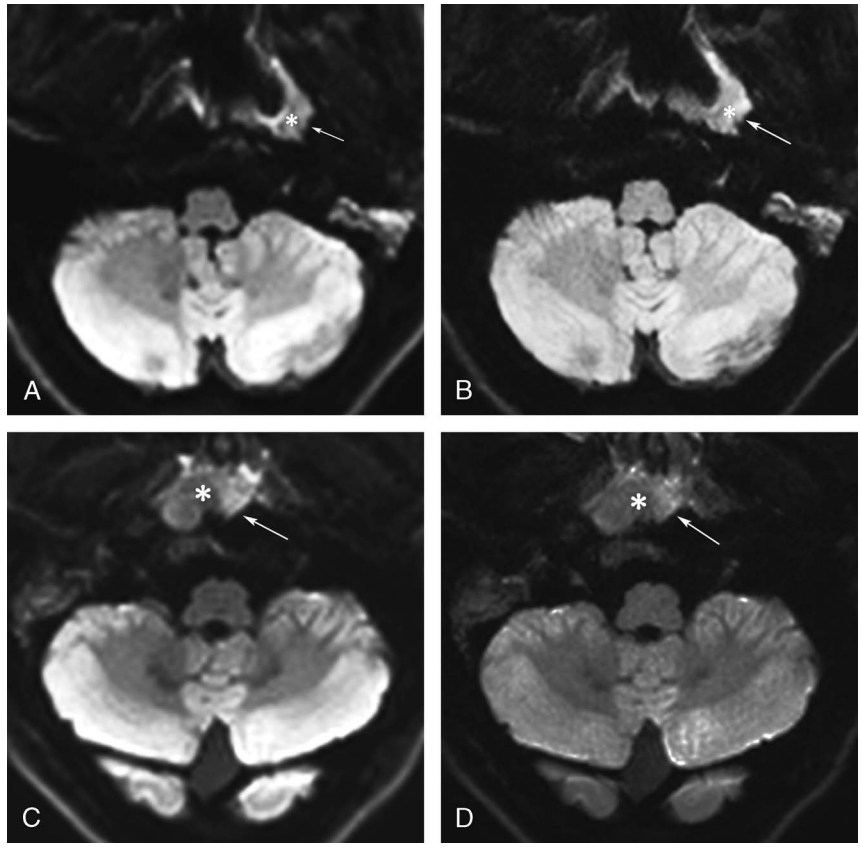

FIGURE 1. Nasopharyngeal carcinoma in a 67-year-old patient and a 53-year-old patient, respectively. Both b800 maps displayed the mass (white star) with restricted diffusion well, whereas compared with RS-DWI (A, C), SMS-RS-DWI (B, D) showed less susceptibility artifacts (white arrow), improved mage quality, and more clearly tumor edge.

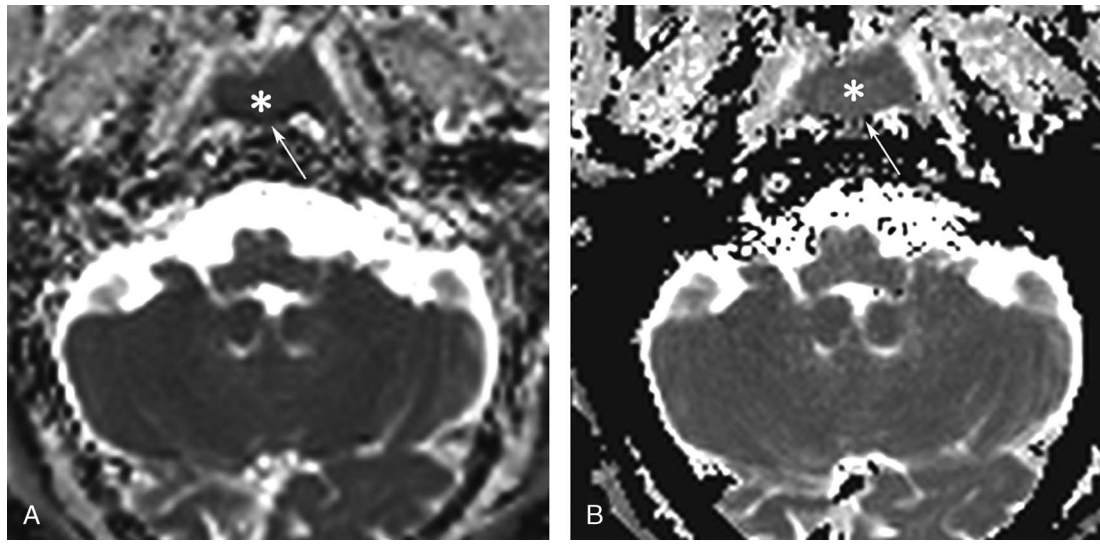

FIGURE 2. A 59-year-old male patient with neoplasm (white star) in the bilateral nasopharyngeal wall (white arrow). The ADC maps of RS-DWI (A) and SMS-RS-DWI (B) show focal low signal intensity in the corresponding region with similar ADC value.

Wilcoxon-Mann-Whitney test was used to analyze the qualitative parameters (overall image quality, tumor edge sharpness, and susceptibility artifacts), and a paired Student *t* test was used to analyze the quantitative parameters (maximum diameter, minimum diameter, maximum tumor area, and ADC value). The anatomic agreement between 2 DWI sequences with T2WI was determined using ICCs (2-way random analysis).[18] The model used absolute agreement options, and the mean measures were selected for further analyses.

RESULTS

The Intraobserver Consistency Analysis

The intraobserver agreements for different qualitative indicators were substantial or excellent, with κ values of 0.689 to 0.871. The intraobserver agreements for various quantitative indicators were all excellent, with κ values greater than 0.8. A detailed summary of consistency analyses for the 4 readers is given separately for qualitative and quantitative image assessments in Tables 2 and 3, respectively.

Scan Time

In the present study, the total scan time was 3 minutes 17 seconds for RS-DWI and 3 minutes 8 seconds for SMS-RS-DWI. For RS-DWI, 15 slices were obtained with a spatial resolution of $1.7 \times 1.7 \times 4$ mm^3. For SMS-RS-DWI, the process was performed with a higher spatial resolution of $1.4 \times 1.4 \times 4$mm^3 and a 2-fold slice number. Thus, SMS-RS-DWI could cover a larger anatomic region with similar scan time.

Qualitative and Quantitative Image Assessments

With the pooled data from all readers, the SMS-RS-DWI had better overall image quality (3.40 ± 0.53 vs 2.71 ± 0.48; $P < 0.05$) with improved tumor edge sharpness than RS-DWI (3.29 ± 0.65 vs 2.64 ± 0.47; $P < 0.05$). Susceptibility artifacts were reduced with SMS-RS-DWI and thus had lower scores than RS-DWI (0.85 ± 0.57 vs 1.36 ± 0.57; $P < 0.05$). Representative images showing image quality improvements in NPC are provided in Figure 1. The mean maximum diameter, mean minimum diameter, and mean maximum tumor area measured from SMS-RS-DWI showed no significant differences compared with those of RS-DWI (all $P > 0.05$). The mean ADC values of SMS-RS-DWI and RS-DWI were $737.20 \pm 136.42 \times 10^{-6}$ and $746.57 \pm 142.05 \times 10^{-6}$ mm^2/s, respectively, and were not significantly different ($P = 0.980$; Fig. 2). The detailed results are shown in Table 4.

TABLE 4. Qualitative and Quantitative Evaluation of SMS-RS-DWI and RS-DWI

Parameter	RS-DWI	SMS-RS-DWI	*P*
Overall image quality*	2.71 ± 0.48	3.40 ± 0.53	**<0.0001**†
Sharpness of tumor edges‡	2.64 ± 0.47	3.26 ± 0.56	**<0.0001**†
Susceptibility artifacts§	1.36 ± 0.57	0.85 ± 0.57	**<0.0001**†
Maximum diameter, mm	25.54 ± 10.03	25.93 ± 9.95	0.822‖
Minimum diameter, mm	15.99 ± 5.68	16.70 ± 7.72	0.582‖
Maximum tumor area, mm^2	469.30 ± 41.88	494.46 ± 44.89	0.537‖
ADC value	746.57 ± 142.05	737.20 ± 136.42	0.980‖

Data are mean scores ± SDs.

The statistically significant *P* value is shown in bold.

*Five-point Likert scale from 0 (nondiagnostic) to 4 (excellent).

†Wilcoxon-Mann-Whitney test.

‡Five-point Likert scale from 0 (no identification) to 4 (excellent differentiation of lesion borders).

§Five-point Likert scale from 0 (no artifacts) to 4 (very severe artifacts that prevents the diagnostic assessment of the lesion).

‖Paired Student *t* test.

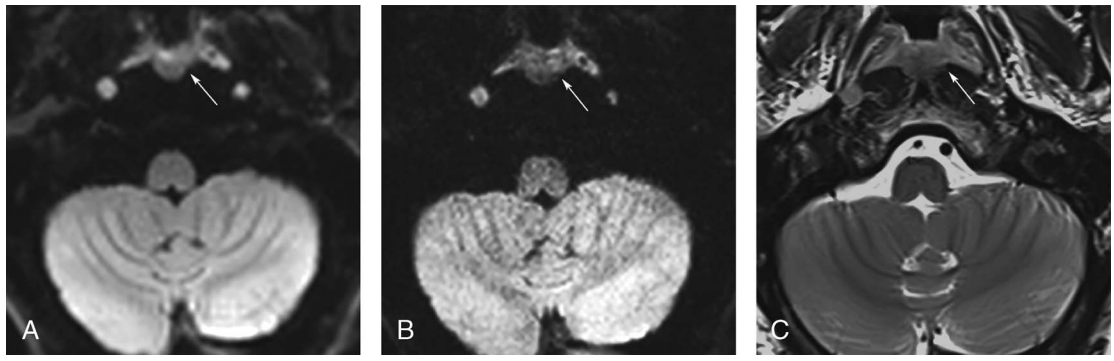

FIGURE 3. At the same level, RS-DWI (A), SMS-RS-DWI (B), and TSE-T2WI (C) show a mass that mainly involved the nasopharynx (white arrow). There is almost no distortion observed on DWI compared with T2WI.

Image Distortion Analysis

To evaluate the image distortion, the relative differences between DWI and T2WI were calculated using the following formula:

$$|M_{\mathrm{DWI}} - M_{\mathrm{T2WI}}| / M_{\mathrm{T2WI}}$$

where M stand for maximum diameter, minimum diameter, or area of the tumor in the maximum slice.

For RS-DWI, the relative differences in maximum diameter, minimum diameter, and maximum tumor area in relation to T2WI were 0.09 ± 0.08 for the maximum diameter, 0.13 ± 0.11 for the minimum diameter, and 0.14 ± 0.12 for the maximum tumor area, respectively. There was no significant overestimation or underestimation of the tumor size by the RS-DWI ($P > 0.05$; Fig. 3). For the SMS-RS-DWI, the relative differences in the quantitative measurements in relation to the T2WI imaging were all lower than those of RS-DWI. The maximum diameter, minimum diameter, and maximum tumor area were 0.08 ± 0.07, 0.11 ± 0.08, and 0.12 ± 0.09, respectively. There was no significant overestimation or underestimation of the tumor size by SMS-RS-DWI ($P > 0.05$). The results of the quantitative evaluations are shown in Table 5.

Considering the anatomic agreements between the 2 RESOLVE sequences with T2WI measured using ICCs, SMS-RS-DWI with T2WI yielded slightly higher agreements than RS-DWI with T2WI for the maximum diameter (ICCs, 0.975 vs 0.973), minimum diameter (0.977 vs 0.974), and maximum tumor area (0.986 vs 0.982). The results of the agreements between RS-DWI and SMS-RS-DWI with T2WI are summarized in Table 6.

DISCUSSION

In the current study, all images were evaluated by 4 independent readers (2 junior radiologists and 2 senior radiologists). The measurement consistency between the radiologists of different seniority demonstrated substantial or excellent agreement, which confirmed the feasibility and reliability of the evaluation methods in our research.

In the head and neck region, the optimization of DWI techniques to improve image quality and reduce total scan time is significantly important for accurate diagnosis and increasing patient throughput. The SMS sequences acquire several images during each repetition time using multiband composite radiofrequency pulses, causing a simultaneous excitation of multiple image planes.[19] Readout-segmented echo-planar DWI was used to sample subsets of k-space points in the readout direction, and the usage of 2D navigator-echo acquisition and parallel imaging enabled a nonlinear phase correction to control the real-time reacquisition of unusable data that were not corrected.[11] The SMS technique was proposed to increase the acquisition efficiency, and the RS technique could produce high-spatial-resolution DWI images. In the present study, SMS and RS techniques were combined for preferable data acquisition.

This study proved that SMS-RS-DWI was superior to RS-DWI with regard to overall image quality and lesion conspicuity, which were consistent with a previous study on breast imaging.[20] Moreover, a prospective study evaluated the SMS RS-EPI sequence with 4 *b* values in breast lesions and reported that SMS RS-EPI could significantly reduce the acquisition time and produce similar diagnostic performances compared with the conventional RS-EPI.[21] However, Su et al[17] showed that the overall image quality, evaluated in healthy volunteers, showed no significant differences between conventional RESOLVE and the prototypic SMS-RESOLVE, which could be due to discrepancies in detecting small deviations. In that study, the SMS technique performed better in the images with existing lesions compared with those with normal structures. Lesion identification from the patients' images was

TABLE 5. Quantitative Evaluation of SMS-RS-DWI and RS-DWI Versus T2WI

Parameter	RS-DWI	T2WI	Relative Difference	*P*
Maximum diameter, mm	25.54 ± 10.03	27.41 ± 10.12	0.09 ± 0.08	0.387
Minimum diameter, mm	15.99 ± 5.68	16.11 ± 6.07	0.13 ± 0.11	0.945
Maximum tumor area, mm^2	469.30 ± 41.88	501.9 ± 42.91	0.14 ± 0.12	0.715
	SMS-DWI	**T2WI**	**Relative Difference**	***P***
Maximum diameter, mm	25.93 ± 9.95	27.41 ± 10.12	0.08 ± 0.07	0.493
Minimum diameter, mm	16.70 ± 7.72	16.11 ± 6.07	0.11 ± 0.08	0.726
Maximum tumor area, mm^2	494.46 ± 44.89	501.9 ± 42.91	0.12 ± 0.09	0.925

TABLE 6. Anatomic Agreement of SMS-RS-DWI and RS-DWI With T2WI Measured by ICCs

Parameter		RS-DWI	SMS-RS-DWI
Maximum diameter, mm	ICC	0.973	0.975
	95% CI	0.950–0.985	0.955–0.983
Minimum diameter, mm	ICC	0.974	0.977
	95% CI	0.953–0.986	0.958–0.988
Maximum tumor area, mm^2	ICC	0.982	0.986
	95% CI	0.968–0.990	0.974–0.992

CI indicates confidence interval.

comparable between the 2 DWI techniques. The limited image quality due to signal losses in the lower neck region influenced the total image analyses. Our study focused on NPC, and the effective coil density remained stable in the upper neck region; therefore, the image signal densities were stable among different patients.

In addition, SMS-RS-DWI showed fewer susceptibility artifacts than RS-DWI in this study. At the base of the skull, adjacent organs were not distinguished because of magnetic susceptibility artifacts caused by susceptibility changes at tissue-air and tissue-bone interfaces, T2* blurring, and low spatial resolution interference with reduced image quality. Simultaneous multislice resolved these issues using an improved in-plane resolution resulting in higher spatial resolution and less partial volume effect. Moreover, SMS-RS-DWI has a smaller bandwidth than RS-DWI (694 vs 963 Hz/px); therefore, the broadband-like artifact caused by increased noise amplification was more severe in RS-DWI than in SMS-RS-DWI. In recent studies, SMS was widely used in abdominal imaging. Tavakoli et al[15] performed an SMS-DWI sequence with respiratory triggering (RT), which yielded a substantial reduction of motion and susceptibility artifacts in the liver. Furthermore, the pancreas consistently displayed more clearly, suggesting that SMS-RT-DWI is superior to standard DWI for detecting small pancreatic lesions. Another study showed that SMS-RT-DWI could improve the image quality of the kidneys with fewer imaging artifacts, giving a better depiction of various renal tumors and pyelonephritis.[22]

Several studies proved that SMS-RS-EPI was comparable with conventional RS-EPI in yielding similar signal-to-noise ratios at markedly reduced scan time. For SMS-RS-EPI with slice acceleration factor 2, the average image acquisition time was decreased by 40% to 48.6% compared with that of RS-EPI.[17,20,21,23] In our study, SMS-RS-DWI could cover a doubled anatomic region with a similar scan time compared with RS-DWI. In previous studies, the DWI characteristics of NPC were closely correlated with different tumor stages.[24] Diffusion-weighted imaging also proved useful in detecting 5- to 10-mm metastatic lymph nodes in NPC patients.[25] These findings have demonstrated the function of DWI in pretreatment staging of NPC patients. The detection of tumor extension and metastatic lymph nodes also plays an essential role in treatment strategies of NPC determined by the TNM staging system. In the current cohort, 9 patients have pathologically

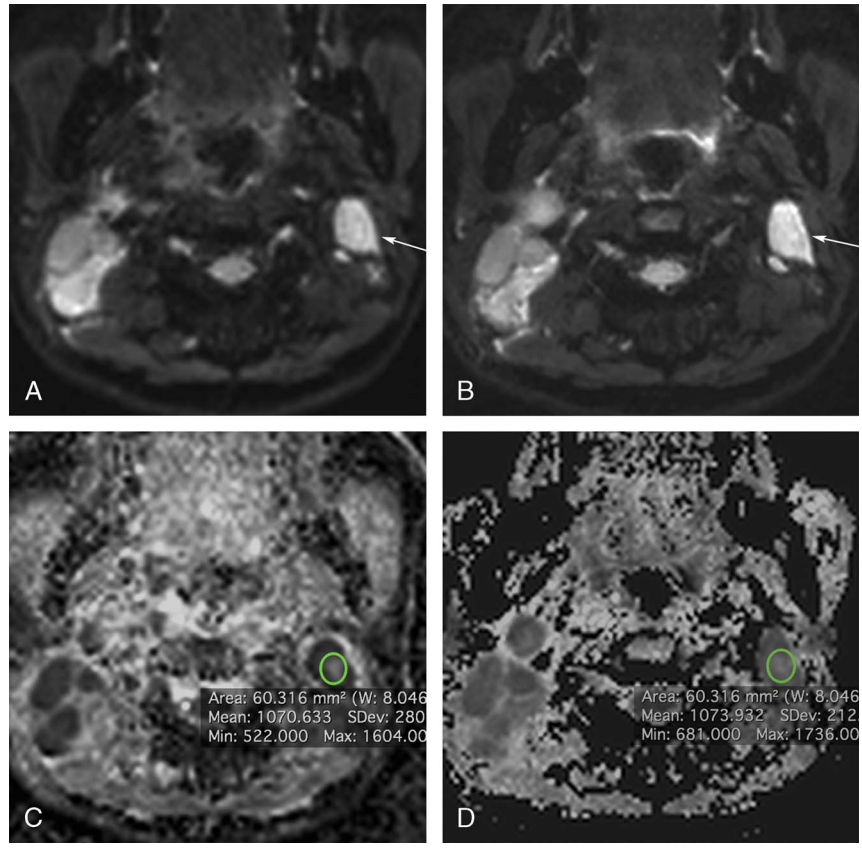

FIGURE 4. A 42-year-old male patient with diagnosed NPC and bilateral cervical lymph node enlargement. The left level II cervical lymph node was proved metastasis by biopsy pathology (white arrow). The SMS-RS-DWI technique (B) shows improved image quality and more clearly lesion edge compared with RS-DWI (A). The ADC maps of RS-DWI (C) and SMS-RS-DWI (D) show focal low signal intensity of the given lymph node with similar ADC value (green circle). Figure 4 can be viewed online in color at www.jcat.org.

proven metastatic lymph nodes, and RS-DWI and SMS-RS-DWI imaging showed the nodal disease available in these patients (Fig. 4). For the lack of the biopsy-proven lymphadenopathy in all patients, the systematic evaluation of the lymph nodes could not be effectively achieved. Future studies with more pathologically proven lymph nodes should be conducted to assess the feasibility and superiority of SMS-RS-DWI in detecting metastatic lymph nodes. The more extensive scan coverage enhanced the clinical feasibility of SMS-RS-DWI sequences. Although we did not perform the related experiment in the current study, it will take only about 6 minutes for SMS-RS-DWI to cover the whole head-neck region for TNM staging, whereas for RS-DWI, it needs about 12 minutes. A 6-minute sequence is relatively acceptable in clinical practice concerning patient compliance. Previous studies have reported that the ADC values were useful to distinguish NPC from NPL or benign hyperplasia.[3,26,27] These values could also predict the risk of distant metastases, curative effects of neoadjuvant chemotherapy,[4] and long-term clinical outcomes[6] in patients with NPC.[28] In our study, the ADC values did not differ significantly between SMS-RS-DWI and the routine RS-DWI.

The present study has some limitations. First, the scan time of SMS-RS-DWI was still longer than that required for standard SS-EPI. Further optimization of the acceleration factors, or combination with other acceleration techniques, such as compressed sensing, should be undertaken to resolve these issues. Second, although SMS-RS-DWI could achieve a double coverage or more, compared with RS-DWI with the same scan time, we did not include the whole neck to evaluate the suspicious lymph nodes. Third, the appearance of metastatic lymph nodes with SMS-RS-DWI sequences would be of great clinical interest; therefore, more patients with pathologically proven metastatic lymph nodes, especially the 5- to 10-mm small lymph nodes, will be enrolled for more comprehensive evaluation. Future studies with a larger sample size should be conducted to include this clinically important application, as well as monitoring treatment responses and grading tumors, and others.

In conclusion, SMS-RS-DWI can significantly improve image quality with more extensive anatomic coverage in patients with NPC and has comparable scan times with routine RS-DWI. The SMS-RS-DWI technique is useful for clinical application in head and neck imaging to increase the accuracy of diagnosis. Further studies are required to investigate the ability of the SMS technique to assess large coverage and identify more metastatic lymph nodes.

REFERENCES

1. Chen YP, Chan ATC, Le QT, et al. Nasopharyngeal carcinoma. *Lancet*. 2019;394:64–80.
2. Bray F, Ferlay J, Soerjomataram I, et al. Global cancer statistics 2018: GLOBOCAN estimates of incidence and mortality worldwide for 36 cancers in 185 countries. *CA Cancer J Clin*. 2018;68:394–424.
3. Ai QY, King AD, Chan JSM, et al. Distinguishing early-stage nasopharyngeal carcinoma from benign hyperplasia using intravoxel incoherent motion diffusion-weighted MRI. *Eur Radiol*. 2019;29:5627–5634.
4. Chen Y, Liu X, Zheng D, et al. Diffusion-weighted magnetic resonance imaging for early response assessment of chemoradiotherapy in patients with nasopharyngeal carcinoma. *Magn Reson Imaging*. 2014;32:630–637.
5. Zheng D, Lai G, Chen Y, et al. Integrating dynamic contrast-enhanced magnetic resonance imaging and diffusion kurtosis imaging for neoadjuvant chemotherapy assessment of nasopharyngeal carcinoma. *J Magn Reson Imaging*. 2018;48:1208–1216.
6. Law BK, King AD, Bhatia KS, et al. Diffusion-weighted imaging of nasopharyngeal carcinoma: can pretreatment DWI predict local failure based on long-term outcome? *Am J Neuroradiol*. 2016;37:1706–1712.
7. Mao J, Shen J, Yang Q, et al. Intravoxel incoherent motion MRI in differentiation between recurrent carcinoma and postchemoradiation fibrosis of the skull base in patients with nasopharyngeal carcinoma. *J Magn Reson Imaging*. 2016;6:1556–1564.
8. Wang C, Liu L, Lai S, et al. Diagnostic value of diffusion-weighted magnetic resonance imaging for local and skull base recurrence of nasopharyngeal carcinoma after radiotherapy. *Medicine (Baltimore)*. 2018;34:e11929.
9. Koyasu S, Iima M, Umeoka S, et al. The clinical utility of reduced-distortion readout-segmented echo-planar imaging in the head and neck region: initial experience. *Eur Radiol*. 2014;24:3088–3096.
10. Zhao M, Liu Z, Sha Y, et al. Readout-segmented echo-planar imaging in the evaluation of sinonasal lesions: a comprehensive comparison of image quality in single-shot echo-planar imaging. *Magn Reson Imaging*. 2016;34:166–172.
11. Porter DA, Heidemann RM. High resolution diffusion-weighted imaging using readout-segmented echo-planar imaging, parallel imaging and a two-dimensional navigator-based reacquisition. *Magn Reson Med*. 2009;62:468–475.
12. Huang WY, Li MM, Lin SM, et al. In vivo imaging markers for prediction of radiotherapy response in patients with nasopharyngeal carcinoma: RESOLVE DWI versus DKI. *Sci Rep*. 2018;8:15861.
13. Setsompop K, Gagoski BA, Polimeni JR, et al. Blipped-controlled aliasing in parallel imaging for simultaneous multislice echo planar imaging with reduced g-factor penalty. *Magn Reson Med*. 2012;67:1210–1224.
14. Frost R, Jezzard P, Douaud G, et al. Scan time reduction for readout-segmented EPI using simultaneous multislice acceleration: diffusion-weighted imaging at 3 and 7 tesla. *Magn Reson Med*. 2015;74:136–149.
15. Tavakoli A, Attenberger UI, Budjan J, et al. Improved liver diffusion-weighted imaging at 3 T using respiratory triggering in combination with simultaneous multislice acceleration. *Invest Radiol*. 2019;54:744–751.
16. Taron J, Martirosian P, Kuestner T, et al. Scan time reduction in diffusion-weighted imaging of the pancreas using a simultaneous multislice technique with different acceleration factors: how fast can we go? *Eur Radiol*. 2018;28:1504–1511.
17. Su T, Chen Y, Zhang Z, et al. Optimization of simultaneous multislice, readout-segmented echo planar imaging for accelerated diffusion-weighted imaging of the head and neck: a preliminary study. *Acad Radiol*. 2020;27:e245–e253.
18. Thierfelder KM, Scherr MK, Notohamiprodjo M, et al. Diffusion-weighted MRI of the prostate: advantages of Zoomed EPI with parallel-transmit-accelerated 2D-selective excitation imaging. *Eur Radiol*. 2014;24:3233–3241.
19. Feinberg DA, Setsompop K. Ultra-fast MRI of the human brain with simultaneous multi-slice imaging. *J Magn Reson*. 2013;229:90–100.
20. Song SE, Woo OH, Cho KR, et al. Simultaneous multislice readout-segmented Echo planar imaging for diffusion-weighted MRI in patients with invasive breast cancers. *J Magn Reson Imaging*. 2021;53:1108–1115.
21. Hu Y, Zhan C, Yang Z, et al. Accelerating acquisition of readout-segmented echo planar imaging with a simultaneous multi-slice (SMS) technique for diagnosing breast lesions. *Eur Radiol*. 2021;31:2667–2676.
22. Tavakoli A, Krammer J, Attenberger UI, et al. Simultaneous multislice diffusion-weighted imaging of the kidneys at 3 T. *Invest Radiol*. 2020;55:233–238.
23. Filli L, Ghafoor S, Kenkel D, et al. Simultaneous multi-slice readout-segmented echo planar imaging for accelerated diffusion-weighted imaging of the breast. *Eur J Radiol*. 2016;85:274–278.
24. Lai V, Li X, Lee VH, et al. Nasopharyngeal carcinoma: comparison of diffusion and perfusion characteristics between different tumour stages using intravoxel incoherent motion MR imaging. *Eur Radiol*. 2014;24:176–183.

25. Jin GQ, Yang J, Liu LD, et al. The diagnostic value of 1.5-T diffusion-weighted MR imaging in detecting 5 to 10 mm metastatic cervical lymph nodes of nasopharyngeal carcinoma. *Medicine (Baltimore)*. 2016; 95:e4286.

26. Fong D, Bhatia KS, Yeung D, et al. Diagnostic accuracy of diffusion-weighted MR imaging for nasopharyngeal carcinoma, head and neck lymphoma and squamous cell carcinoma at the primary site. *Oral Oncol*. 2010;46:603–606.

27. Wang YJ, Xu XQ, Hu H, et al. Histogram analysis of apparent diffusion coefficient maps for the differentiation between lymphoma and metastatic lymph nodes of squamous cell carcinoma in head and neck region. *Acta Radiol*. 2018;59:672–680.

28. Ai QY, King AD, Law BK, et al. Diffusion-weighted imaging of nasopharyngeal carcinoma to predict distant metastases. *Eur Arch Otorhinolaryngol*. 2017;274:1045–1051.